Pushing Adenosine and ATP SELEX for DNA Aptamers with Nanomolar Affinity

Yuzhe Ding and Juewen Liu*

Department of Chemistry, Waterloo Institute for Nanotechnology

University of Waterloo, Waterloo, Ontario, N2L 3G1, Canada

E-mail: liujw@uwaterloo.ca

Abstract: The classical DNA aptamer for adenosine and ATP has been the most used small molecule binding aptamer for biosensing, imaging and DNA nanotechnology. This sequence has recurred multiple times in previous aptamer selections, and all previous selections used a high concentration of ATP as the target. Herein, two separate selections were performed using adenosine and ATP as targets, respectively. By pushing the target concentrations down to the low micromolar range, two new aptamers with K_d as low as 230 nM were obtained, showing around 30-fold higher affinity compared to the classical aptamer. The classical aptamer sequence still dominated the library in the early rounds of the selections, but they were suppressed in the later rounds. The new aptamers bind to one target molecule instead of two. Mutation studies confirmed their secondary structures and specific binding. Using the deep sequencing data from the selections, long-standing questions such as the existence of one-site aptamers and mutation distribution in the classical aptamer were addressed. Comparisons were made with previously reported DNA aptamers for ATP. Finally, a strand-displacement biosensor was tested showing selectivity for adenosine and its nucleotides.

Introduction

In the aptamer field,[1-3] the adenosine and ATP binding aptamers are among the most studied and used not only in biochemistry but also for analytical, biomedical and nanotechnology applications.[4-9] In 1993, Sassanfar and Szostak isolated an ATP-binding RNA aptamer (K_d ~0.7 μM), which can also bind adenosine.[10] In 1995, using the same ATP column, Huizenga and Szostak reported a DNA aptamer that can bind adenosine and ATP (K_d ~6 μM adenosine).[11] Later, NMR studies showed that the RNA aptamer binds one target molecule,[12-14] whereas the DNA aptamer binds two.[15] Despite this difference in binding

stoichiometry, these two aptamers have some similarities in the way of target binding in terms of non-canonical G·A (the A being the target molecule) base pairing and its stacking with G·G pairs.

Over the last two decades, ATP has been used as a target by many groups to test new aptamer selection methods.[4] A very popular method is to immobilize nucleic acid libraries and use free target molecules for selections.[16-21] For example, Nutiu and Li used the library immobilization method, but obtained the exact same classical DNA aptamer.[17] The other reported aptamers were much less studied or used likely due to their lower affinities, longer sequences, less well-defined structures or containing modified nucleotides.[22-25] All reported DNA aptamers have K_d values higher than 6 μM for adenosine and ATP.

Interestingly, no one used adenosine as a target for selection and all the previous work used ATP.[10, 11, 17, 22-25] The interest in ATP stems from its biological importance. Aside from its role as the major energy currency in cells, ATP is also a biomarker for cancer and other diseases.[26] Being a major signaling nucleoside, adenosine is a highly important molecule as well with functions such as the regulation of sleep and stress.[27, 28] Without the highly negatively charged triphosphate group, adenosine selections may result in new aptamers with stronger affinities.

In this work, we respectively used adenosine and ATP as targets to select new DNA aptamers using the library immobilization method.[16, 17, 19] While we also observed the classical aptamer in both selections, new aptamers with higher binding affinities emerged when we pushed the selections with increased stringency by lowering target concentrations. The growth of new aptamers also suppressed the classical aptamer.

Results and Discussion

Aptamer selections using adenosine and ATP as targets. To select aptamers, we immobilized a DNA library containing a 36-nucleotide random region (N_{36}) by hybridization it to a biotinylated DNA attached to streptavidin-coated beads (Figure S1, Table S1 for DNA sequences).[29, 30] The initial library contained 500 pmol (~3×10^{14}) random DNA sequences. When adenosine or ATP was added, aptamer sequences were released, collected, and amplified by PCR. For the adenosine selection, the adenosine concentration was gradually decreased from 5 mM to 1 μM over a total of 13 rounds (Table S2). The PCR products from round 3, 6, 8, 9, 10, 11, and 13 were deep sequenced. A total of 30073 sequences were obtained from the round 13 library. We analyzed the top ten most abundant sequences, and they can be separated

in two families (Figure 1A). The sequences in family 1 (represented by Ade1301) have two conserved regions marked in red. We used these conserved regions to search for the entire library, and family 1 represented 40.4% of the round 13 sequences. The family 2 sequences (represented by Ade1304) also have two conserved regions (blue/purple nucleotides in Figure 1A), and they represented 3.8% of the round 13 sequences (Figure 1C).

We then searched the two families from the other rounds and found that the family 1 sequences gradually increased over the selection rounds (Figure 1C, red bars). The family 2 sequences also increased but were overall much less compared to family 1 (Figure 1C, blue bars). We also searched for the classical aptamer sequence (containing GGGGA and GGAGGA) in the libraries. Its abundant peaked at round 6 (Figure 1C, black bars), after which it gradually dropped to only ~0.5% in round 13. This result can be explained by the low affinity of this classical aptamer (K_d ~6 μM). When we dropped the adenosine concentration to below 10 μM, it was suppressed.

For the ATP selection, we started with 1 mM ATP and stopped at 10 μM over a total of ten rounds. We deep sequenced the PCR products from round 5, 6, 9, and 10. A total of 64769 sequences were obtained from the round 10 selection. Interestingly, the top ten most abundant sequences (named ATP1001 to ATP1010) also belong to the above two adenosine families, although relatively more family 2 sequences were present. For ATP round 10, family 1 accounted for 51.3% and family 2 reached 9.5% (Figure 1B and 1D). In the ATP selection, the abundance of the classical adenosine aptamer peaked in round 6 (38.0%) and decreased to 11.1% in round 10 (Figure 1D, black bars).

The two new aptamers have longer conserved regions (12+4=16 for Ade1301, 9+7=16 for Ade1304) compared to the classical aptamer (6+6=12). The longer the conserved sequences, the lower the abundance in the initial pool, which may explain the dominance of the classical aptamer in the early rounds. Recurrence of the same functional motifs was also observed in other selections such as repeated discovery of the 8-17 DNAzyme.[31, 32] Our ATP and adenosine selections resulted in the same sequences (only differ by the relative abundance of the two families), suggesting that under our selection conditions, aptamer binding occurred mainly in the adenosine part. This is reasonable since the nucleobase can have more types of interactions with aptamers including hydrogen bonding and π-π stacking.[13-15, 33]

By comparing the relative sequence abundance of the two selections at round 6, the ATP selection had more new aptamers, and this can be attributed to the use of lower ATP concentrations in the early rounds. For the selection by Huizenga and Szostak, a constant ATP concentration of 3 mM was used to yield the classical aptamer.[11] For here, had we stopped at round 6 for the adenosine selection (0.5 mM

adenosine), we would have isolate the classical aptamer again as well. Although Nutiu and Li used a low target concentration of 0.1 mM ATP to finish their selections, they had two random regions (N_{10} and N_{20}) linked by a constant region in their library design.[17] Such a design may disfavor the evolution of the new aptamers (e.g. the middle region needs to form a hairpin structure, *vide infra*). This may explain the dominance of the classical sequence in their selection.

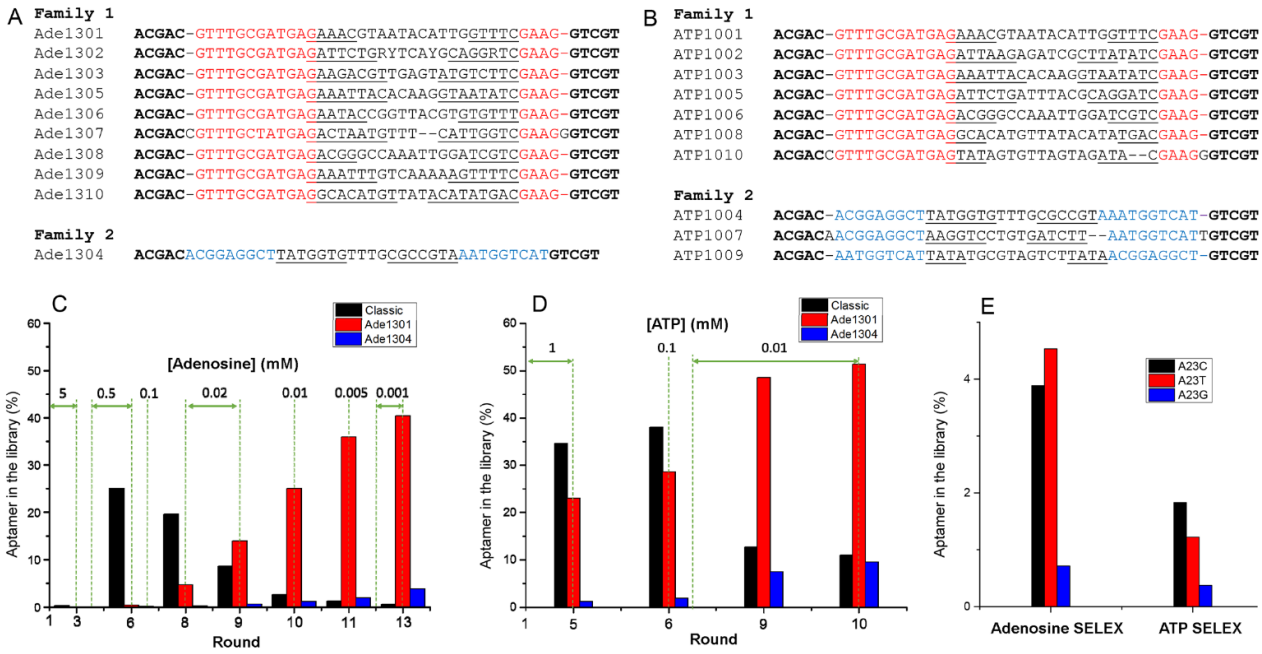

Figure 1. Alignment of the top 10 most abundant sequences in the final round of (A) the adenosine and (B) the ATP selections. The nucleotides marked in red and blue are the conserved regions of the aptamers. The N_{36} regions are in the middle, and we only kept five extra nucleotides on each end (in boldface) that can pair with each other. The abundance of the top sequences in different rounds of (C) the adenosine and (D) the ATP selections. (E) The abundance of a few mutated sequences at the 23rd position of the classical aptamer in round 6 of the two selections.

New aptamers with nanomolar affinities. For the adenosine selection, while over 40% of the round 13 sequences belong to family 1, the most abundant sequence Ade1301 had only 543 copies (1.8%) of the library. The Mfold[34] predicted secondary structure of Ade1301 is shown in Figure 2A, where the conserved nucleotides are colored in red, and the rest of the nucleotides from the random region can fold in a hairpin. We also checked the other top sequences and they also have such a hairpin structure (the stem region underlined, Figure 1A). Therefore, having a hairpin structure is important, although the

sequence of the hairpin is less important. The secondary structure of Ade1304 is shown in Figure 2B, which also has two conserved regions colored in blue connected by a hairpin.

To measure the binding affinity of the selected aptamers, we used isothermal titration calorimetry (ITC).[35, 36] We titrated 400 μM adenosine into 10 μM Ade1301 aptamer in the selection buffer. The ITC traces and integrated heat are shown in Figure 2E, and the exothermic binding can be seen from the downward spikes. The K_d value was fitted to be 350 ± 80 nM. To test the role of the hairpin, we deleted the nucleotides in the box and named this truncated sequence Ade1301b (Figure 2A). Ade1301b showed an even lower K_d of 230 nM (Figure S2A Table S3). Since Ade1301b is shorter, our subsequent studies focused on this truncated sequence. We then titrated Ade1301b with ATP (Figure 2F), wherein the heat release decreased nearly by half and the K_d was 2.5 μM. This K_d value is also smaller than that of the classical aptamer for ATP.[11, 37]

We then titrated adenosine into the Ade1304 aptamer, and a K_d of 230 ± 90 nM was obtained (Figure 2G). Since Ade1304 has a long stem, we deleted the boxed nucleotides in green and made a mutant named Ade1304b (Figure 2B), which had a similar K_d of 400 ± 160 nM (Figure S2B). When ATP was titrated into Ade1304b, the K_d was 2.3 μM. For comparison, the classical DNA aptamer (Figure 2C) had a K_d of 8.2 μM adenosine under the same buffer condition (Figure 2H), consistent with the literature.[11] Therefore, the two new aptamers had ~35-fold higher affinity for adenosine than the classical aptamer.

The thermodynamic values from ITC are presented in Table 1. We first noticed that the binding stoichiometry was close to 1 for both Ade1301 and Ade1304. This is in sharp contrast to the binding of two adenosine molecules by the classical aptamer (the last entry in Table 1). Their different sequences, affinities and stoichiometry indicated that we obtained two new aptamers. All the three aptamers can bind both adenosine and ATP. For the same aptamer, binding adenosine released more heat but had more entropy loss compared to binding ATP. The less entropy drop for ATP can be attributed to the phosphate chain still being flexible, also suggesting that binding took place mainly in the adenosine part.

Revisiting the classical aptamer: one-site aptamers and mutants from deep sequencing. This is the first time that deep sequencing was done to generate nearly 10,000 classical aptamer sequences. The two previous selections only yielded less than 100 sequences.[11, 17] We thus took this opportunity to answer some interesting questions regarding the classical aptamer. While the classical DNA aptamer is featured with two identical binding sites, sequences with just one binding site can also bind adenosine with a similar K_d.[37-39] An example of a previously characterized one-site binding aptamer is shown in Figure 2D, where the other binding site was removed by forming extra base pairs. Previous selections did

not show any sequence with such a one-site structure, and the reason remained elusive.[38] We then searched the round 6 sequences of the adenosine selection (Table S4). Indeed, we found one-site aptamers, although at a very low abundance of ~0.7% (312 out of 46239). One of the sequences from the search result was folded and it shows a one-site aptamer similar to that in Figure 2D (Figure S4C). Therefore, the previous selections missed the one-site sequences likely due to its low abundance, but such sequences can be evolved from selections. Since one-site aptamers had even less sequence requirements compared to the classical two-site aptamer, one would expect one-site aptamers to outnumber two-site ones. However, the opposite was observed. It might be that for a library with a long random region, having a very small binding region would pose more requirements for the rest of the sequences (e.g. need to form long base paired regions to consume the sequences).

We further used the sequences to analyze mutations. The A23 position in the classical aptamer (Figure 2C) can be mutated to other three nucleotides as seen in the original selection paper by Szostak.[11] Xiao and coworkers separately modified A23 to thymine, guanine, and cytosine in the classical aptamer and proved the mutants can still bind ATP.[40] Interestingly, the A23T mutant led to better selectivity for adenosine over ATP. We then examined our round 6 adenosine selection library and indeed found all the three point mutations, although their abundance was lower than the classical sequence: A23C (3.9%), A23T (4.5%), and A23G (0.7%) (Figure 1E). Indeed, the A23T mutation had the highest abundance among the three, although they were all much lower than the classical sequence (24.9%). We also searched the round 6 sequences of the ATP selection, in which the A23T mutant (1.2%) was less abundant than A23C (1.8%) (Figure 1E). This was also consistent with the expected selectivity. Therefore, using deep sequencing, we also gained more insights into the classical aptamer.

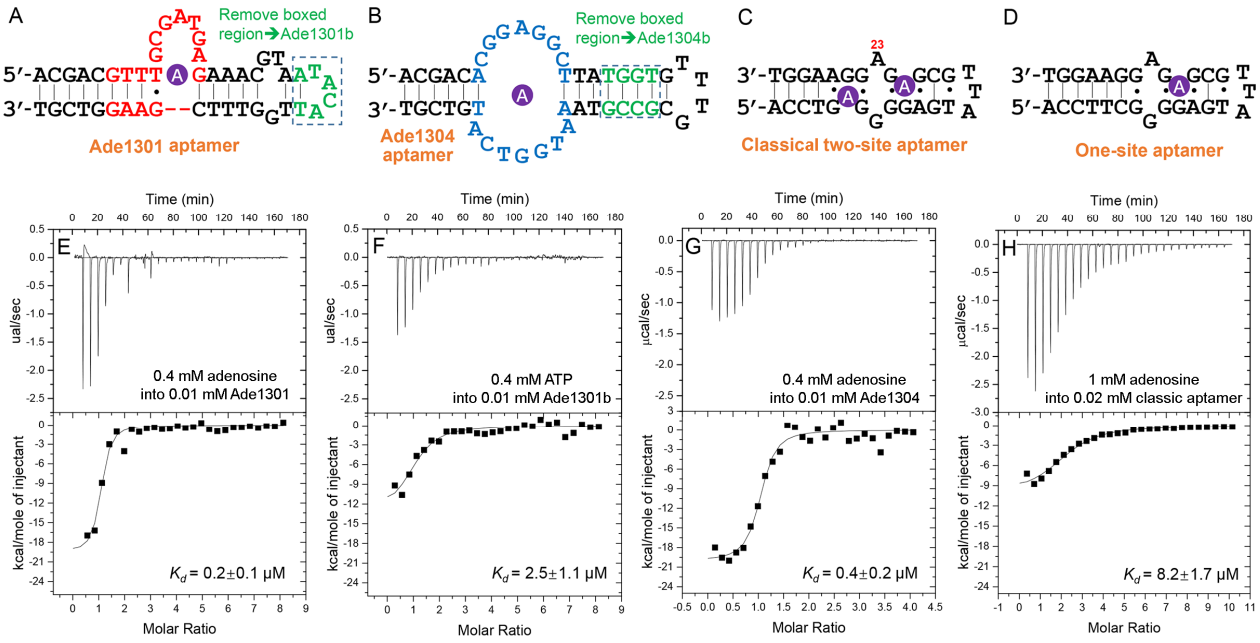

Figure 2. The secondary structure of (A) the Ade1301 (B) the Ade1304, (C) the classical DNA aptamer, and (D) a one-site classical aptamer. In (A, B), the red and green nucleotides are conserved, and the green nucleotides are truncated. The target molecules are represented by the purple A circles. In (C), the adenine in position 23 is marked and this number was based on the literature.[40] ITC analysis of aptamer binding by titrating (E) 400 μM adenosine into 10 μM Ade1301, (F) 400 μM ATP into 10 μM Ade1301b, (G) 400 μM adenosine into 10 μM Ade 1304Ade, and (H) 1 mM adenosine into 20 μM classical DNA aptamer. The buffer contained 50 mM Tris, pH 7.6, 500 mM NaCl, and 20 mM $MgCl_2$.

Table 1. Aptamer binding thermodynamic data from ITC.

Aptamer	Target	*N*	K_d (μM)	Δ*H* (kcal/mol)	Δ*S* (cal/mol/K)
Ade1301b	Ade	0.73 ± 0.03	0.2 ± 0.1	-24.3 ± 1.6	-51.1
Ade1301b	ATP	1.1 ± 0.1	2.5 ± 1.1	- 13.5 ± 2.2	-19.6
Ade1304b	Ade	1.00 ± 0.04	0.4 ± 0.2	-23.1 ± 1.2	-48.7
Ade1304b	ATP	1.04 ± 0.03	2.3 ± 0.4	-18.5 ± 0.8	-36.3
Classical	Ade	2.3 ± 0.1	8.2 ± 1.7	-10.2 ± 0.7	-11

Secondary structure analysis. Since the binding performance for adenosine and ATP was very similar for the two new aptamers selected in this work, and Ade1301 was the dominating sequence, we focused on it in this work. While Ade1301b appeared very different from the classical DNA aptamer, its secondary structure Ade1301b (Figure 3A) has some similarity to the classical RNA aptamer named ATP-40-1 (Figure 3C).[10] For example, the RNA aptamer has an unpaired guanine (G30) and the Ade1301 appeared to have a similar guanine (G32), if this guanine is not in the predicted G·T wobble pair in reality (Figure 3A). Mfold predicted base pairs all the way to this G·T wobble pair, including a G·G mismatch (G6·G35). To test the validity of this structure, we first made a G6C mutation (mutant named Ade1301c) to change the G·G mismatch to a C-G base pair. Interestingly, this change inhibited adenosine binding (Figure 3D), indicating that this GG is not a mismatched pair and thus the downstream base pairs may not be needed for aptamer binding. To test this hypothesis, we then swapped the next two A-T base pairs respectively (Ade1301d and 1301e) and indeed neither showed binding (Figure S2C, D). We further made a G32A mutation in the Ade1301b aptamer (named Ade1301f), which still showed binding and its K_d value increased only 6-fold (Figure 3E). Therefore, this guanine can be mutated to an adenine, and it does not form a wobble pair with T9.

We then turned our attention to the hairpin. We swapped C31 and G17 to produce the Ade1301g mutant, and the K_d decreased only 5-fold (Figure 3F). We further swapped T30 and A18 (Ade1301h) and the K_d value was similar to Ade1301b (Figure 3G, Table S3). Therefore, C31 and G17 formed a base pair. Finally, we cut all DNA base in the blue box in Figure 3A to make Ade1301i, which abolished binding (Figure 3H). Therefore, the hairpin structure cannot be removed, although it can be shortened. The correct secondary structure is shown in Figure 3B, in which the two conserved regions are in two loops. These mutation studies also served as controls to confirm specific aptamer binding. We also noticed that for both the classical DNA and RNA aptamers and the two new aptamers reported here, their conserved regions are rich in purines.

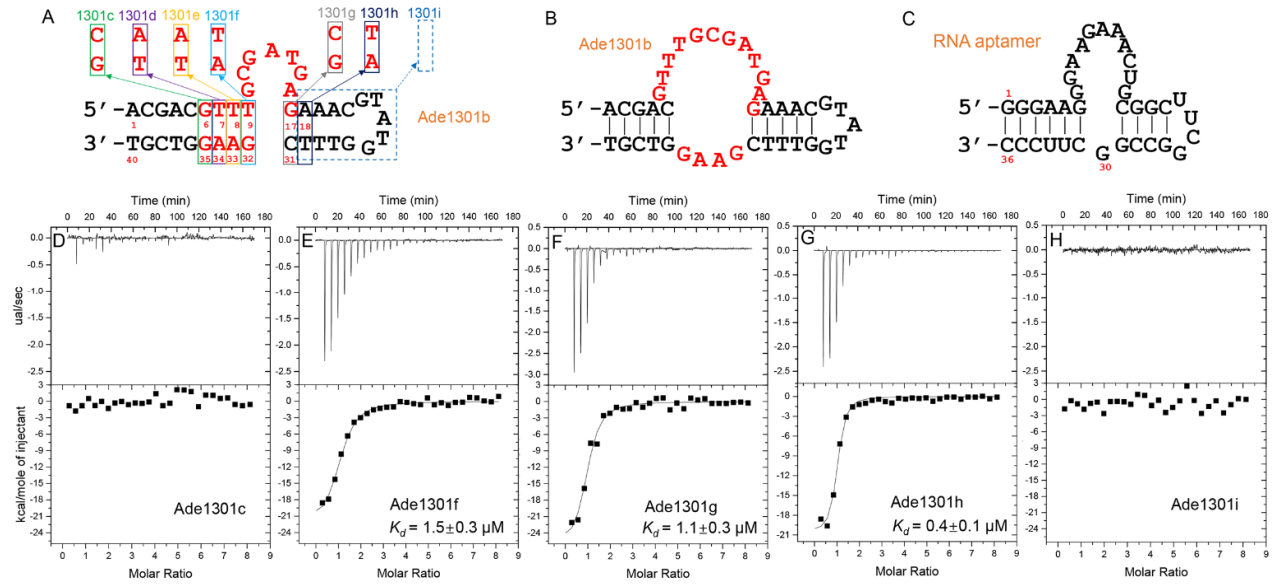

Figure 3. (A) The mutants tested to understand the secondary structure of Ade1301b. The secondary structure of (B) Ade1301b based on the mutation studies. (C) The secondary structure of the classical RNA aptamer. ITC analysis of aptamer binding by titrating 400 μM adenosine into 10 μM (D) Ade1301c, (E) Ade1301f, (F) Ade1301g, (G) Ade1301h, and (H) Ade1301i.

Comparison with previously reported aptamers. ATP has been a popular target for aptamer selection. The only other comparable small molecular target is probably estradiol (selected for at least eight times).[41] Aside from what already been discussed, at least two additional DNA aptamer selections were performed, each used a different selection method.[22, 24] We aligned their sequences with our new aptamers and the classical aptamer, and none of the conserved regions aligned (Figure S3). Their binding properties are compared in Table S4. Most of the previous selection used mM ATP and they did not push for higher affinity aptamers. As a result, their K_d values were also high.

The S10 aptamer was isolated using 4 mM ATP after 14 rounds of selection, but it has almost no structural features (Figure S4).[24] The reported K_d for this aptamer was very high (692 μM), and we did not analyze it further. The other aptamer named ATP-CBA was reported by Qu et al. using flow cytometry,[22] using a library design similar to that by Nutiu and Li.[17] The reported K_d was 26 μM ATP using microscale thermophoresis. We titrated ATP into 10 μM of this aptamer using ITC, and weak binding was observed (Figure S5A,C). When we truncated the aptamer, binding disappeared (Figure S5B,D). So, our observation was consistent with weak binding of ATP with a K_d of 26 μM. The use of modified nucleotides such as threose nucleic acid for selecting ATP aptamers was also reported (K_d 22 μM).[25] Overall, Ade1301b and Ade1304b are new aptamers with higher binding affinities for adenosine and ATP than all previously reported DNA aptamer (Table S5). Their ~200 nM K_d values are already among the lowest in purine binding aptamers obtained from SELEX (e.g., the RNA aptamer for theophylline (100 nM),[42] the RNA aptamer for ATP (700 nM),[10] and the DNA aptamer for theophylline (500 nM),[29] caffeine (2 μM)[30] and uric acid (1 μM)[43]).

Fluorescent sensing of adenosine and ATP. With higher affinity aptamers, we then developed a fluorescent biosensor using the strand-displacement assay.[44] We extended the Ade1301b aptamer by a few nucleotides and labeled it with a FAM fluorophore (Figure 4A). This strand was annealed with a short quencher-labeled strand at a 1:2 ratio to mask the fluorescence. When the aptamer binds adenosine, the binding hairpin structure is formed and the quencher-labeled strand is released leading to increased fluorescence.

To test the sensitivity, different concentrations of adenosine ranging from 0 nM to 500 μM were added to the sensor. Upon adding adenosine, the fluorescence increased immediately (Figure 4B). The higher the adenosine concentration, the stronger the fluorescence increased (Figure 4C). The saturated fluorescence was 2.8-fold higher compared to the background. Based on the relative fluorescence increase (F/F_0) at 10 min, a calibration curve was plotted and an apparent K_d of 19 μM adenosine was fitted. This K_d was 83-fold higher than the K_d value obtained from ITC (0.23 μM), and it can be attributed to the competition from the quencher-labeled strand.[44] The limit of detection (LOD) was calculated to be 1.1 μM based on the signal higher than three times of the standard deviation of background variation.

We further compared the performance of the sensors based on Ade1301b and the classical aptamer using the same design. At the low adenosine concentration region of below 20 μM, the Ade1301b sensor showed a higher sensitivity than classical aptamer. The slope of the Ade1301b sensor is 7-fold higher (Figure 4D), and the LOD of Ade1301b was 13.3-fold lower than the classical aptamer based sensor (14.6 μM). The LOD of our current classical aptamer sensor was also similar to that observed by Nutiu and Li (~25 μM ATP),[44] although the positions of the quencher-labeled strand was slightly different.

For the selectivity test, different concentrations (10 μM, 100 μM, and 1 mM) various nucleosides and nucleotides were added to the Ade1301b sensor, and the relative fluorescence increase $(F-F_0)/F_0$ is shown in Figure 4E. The Ade1301b aptamer showed great specificity for adenosine compared to the other nucleosides including guanosine, thymidine, cytidine, and uridine. While it is not surprising that all the adenosine nucleotides showed fluorescence enhancement, it was interesting to note that the binding decreased following the order of ATP > ADP > AMP. This response is similar to an RNA aptamer obtained after extensive negative selection.[23] It appears that the increasing number of phosphate units helped aptamer binding likely via Mg^{2+} mediated bridging.[45, 46] Finally, the response of adenine was also lower than adenosine, suggesting that the pentose participated in binding. This is also similar to the classical aptamer.[11]

We also tested the selectivity in a 10% human blood serum sample added 100 μM of various nucleosides and nucleotides to the sensor (Figure 4F). Due to the raised background fluorescence from serum, the fold of florescence increased all decreased compared to that in buffer.

Nevertheless, the high selectivity was still retained, indicating that the aptamer can function in biological sample matrix.

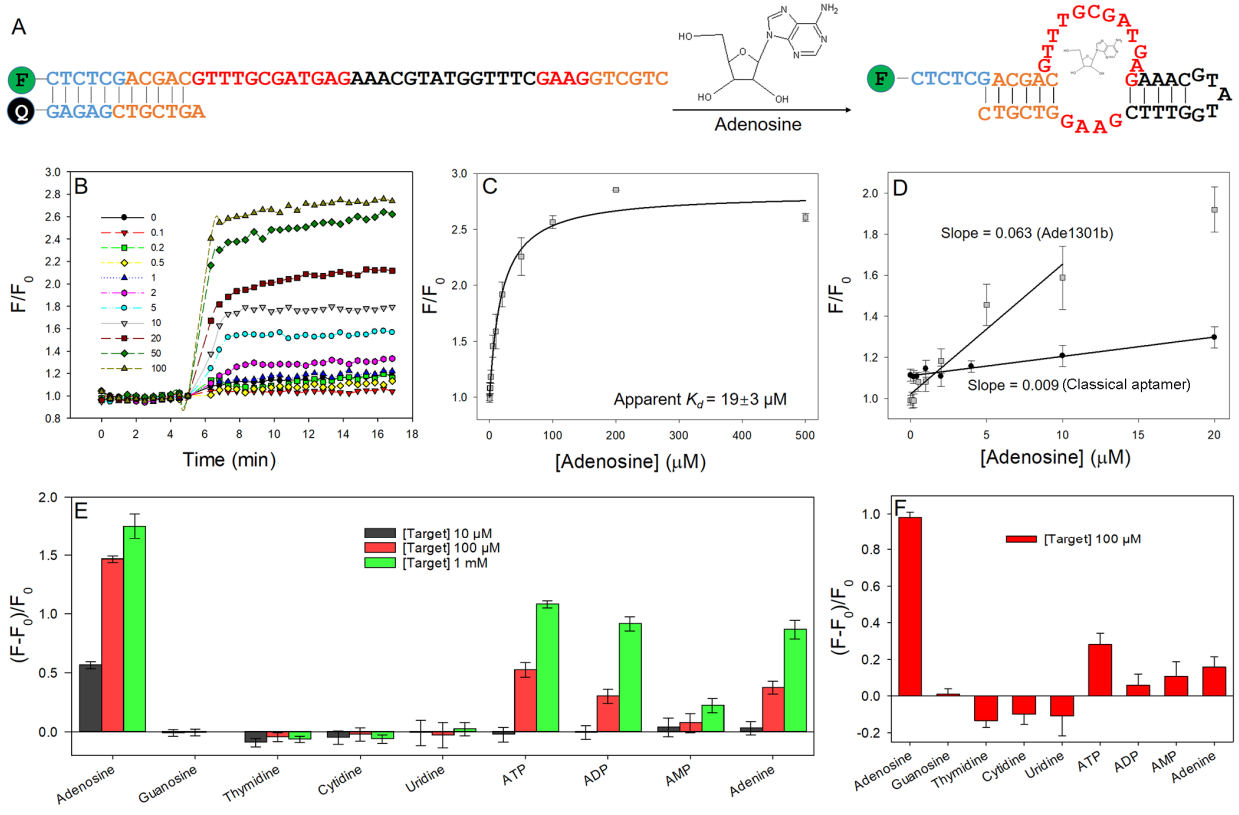

Figure 4. (A) A schematic illustration of the fluorescent sensor for the detection of adenosine. (B) Sensor signaling kinetics in the presence of different concentrations of adenosine in the SELEX buffer. Adenosine was added at 5 min from 0 to 100 μM. (C) Fluorescence intensity increase as a function of adenosine concentration. (D) The linear response at low adenosine concentrations of the Ade1301b and classical aptamer based sensors. (E) The selectivity of the Ade1301b sensor tested at three concentrations. The error bars indicate standard deviation from three independent samples. (F) The Ade1301b sensor selectivity in 10% serum.

Conclusions

In this work, by pushing target concentrations to the low micromolar range, we discovered new and higher affinity DNA aptamers for adenosine and ATP. Their affinities for adenosine were in par with the best in vitro selected aptamers binding to purine derivatives. We have also unified the

understanding of aptamer sequence evolution for these targets. Previous ATP selections stopped at a high target concentration and thus missed the higher affinity sequences. This research indicates the importance of choosing target concentrations in aptamer selectinos.[47, 48] Considering the broad interesting in adenosine/ATP detection, the new aptamers will outperform the previous aptamers in biosensors and other applications. They will give another 30-fold of room for engineering related smart DNA structures and switches compared to the classical aptamer.[49-51] Using the deep sequencing data, statistical analysis was performed to gain insights into the classical aptamer in terms of the number of binding sites and mutations related to selectivity. Since the new aptamers had similar binding affinity and stoichiometry to the RNA aptamers, these new aptamers provide another example to compare RNA and DNA aptamers for binding.

Methods

Chemicals

The DNA samples used in this study were purchased from Integrated DNA Technologies (Coralville, IA, USA, see Table S1 for sequences). Streptavidin agarose resin was purchased from Fisher Scientific. AMP (adenosine monophosphate), guanine, uridine, cytidine, sodium chloride, and magnesium chloride were obtained from Amerseco (Framingham, MA, USA). ATP (adenosine triphosphate), ADP (adenosine diphosphate), thymidine, sodium hydroxide, hydrochloric acid, tris(hydroxymethyl)aminomethane (Tris), and Amicon Ultra-0.5 centrifugal filter unit (3k and 10k molecular weight cut off) were purchased from Millipore-Sigma (Oakville, ON, Canada). Micro bio-spin chromatography columns and SsoFast EvaGreen supermix were from Bio-Rad. dNTP mix, Taq DNA polymerase with ThermoPol buffer, and the low molecular weight DNA ladder were purchased from New England Biolabs (Ipswich, MA, USA). All of the buffers and solutions were prepared with Milli-Q water. SELEX buffer: 50 mM Tris, pH 7.6, 500 mM NaCl, 20 mM $MgCl_2$.

SELEX

The library design (Table S1) and selection method (Figure S1) were based on previous reports of the Stojanovic group[52] with some modifications.[30] We used the same method and library for both

selections. For each round, the single-stranded library was annealed by heating with five times excess of biotinylated capture strand in boiling water for 1 min followed by gradual cooling to room temperature over 30 min in the SELEX buffer. Meanwhile, 288 μL streptavidin agarose resin was loaded into a micro chromatography column and washed five times with 500 μL SELEX buffer. The annealed DNA was passed through the resin six to eight time for binding. After that, the resin was washed 12 times to remove unbound library. After washing, 750 μL of adenosine or ATP solution dissolved in the SELEX buffer was adding and the eluted DNA was collected using the gravity flow. The collected DNA was concentrated by a 3k molecular weight cut off filter and washed by Milli-Q water six times. The final volume of the purified DNA was adjusted to 60 μL using Milli-Q water. Biotinylated reverse prime was used to synthesize 3 mL PCR products, which were purified and concentrated to 250 μL with strand separation buffer (50 mM Tris, pH 7.6, 250 mM NaCl) by using a 10k molecular weight cut off filter. The purified PCR products were mixed with streptavidin agarose resin and washed ten times by the strand separation buffer. Then, 600 μL NaOH (0.2 M) was added into the column and incubated 40 min to elute ssDNA. After neutralization, the concentration of the DNA was quantified by using a Spark microplate reader (Tecan) and it was used for the next round of selection. The concentrations of the library and adenosine or ATP are listed in Table S2.

Isothermal Titration Calorimetry (ITC)

All the ITC experiments were performed on a VP-ITC microcalorimeter instrument (MicroCal). Before each time experiment, the cell chamber and syringe were cleaned by Milli-Q water carefully. DNA aptamers and target molecules were dissolved in the SELEX buffer and then degassed for 5 min before experiment. 1.4 mL aptamer was loaded into the cell chamber and 300 μL target was loaded into the syringe. The titration experiment were carried out at 25°C. Each time, 10 μL target was injected except for the first time injection (2 μL). The time between each injection was 360 s. The final thermodynamic values were obtained by fitting the titration curves to a one-site binding model by using the Origin software.

Sensor Testing

The sensing experiments were performed in a 96-well microplate (λ_{Ex} = 485 nm; λ_{Em} = 525 nm) using a microplate reader (Tecan Spark). 1 μM FAM-labeled Ade1301b aptamer was annealed

with 2 μM quencher-labeled DNA in the SELEX buffer. The final sensor contained 20 nM FAM-labeled strand in 100 μL volume. A small volume of concentrated target molecule was added to trigger sensor response. For detection in serum, human AB serum was diluted into the SELEX buffer to reach a final of 10%, and 100 μM of various target molecules were individually tested.

Supporting Information

The Supporting Information is available free of charge at https://pubs.acs.org/doi/10.1021/jacs.xxxxxx.

Scheme of the SELEX procedures and list of selection conditions; tables showing the DNA sequences used; ITC-based binding thermodynamic constants; statistics of the appearance of potential one-site aptamers; comparison of all literature reported ATP binding aptamers; additional ITC data (PDF)

Acknowledgements

We thank Y. Zhao for helping search DNA sequences and Z. Zhang for a preliminary ITC experiment. Funding for this work was from a Mitacs Accelerate grant and from the Natural Sciences and Engineering Research Council of Canada (NSERC).

References

(1) Famulok, M.; Hartig, J. S.; Mayer, G., Functional Aptamers and Aptazymes in Biotechnology, Diagnostics, and Therapy. *Chem. Rev.* **2007**, 107, 3715-3743.
(2) Yu, H.; Alkhamis, O.; Canoura, J.; Liu, Y.; Xiao, Y., Advances and Challenges in Small-Molecule DNA Aptamer Isolation, Characterization, and Sensor Development. *Angew. Chem. Int. Ed.* **2021**, 60, 16800-16823.
(3) Wu, L.; Wang, Y.; Xu, X.; Liu, Y.; Lin, B.; Zhang, M.; Zhang, J.; Wan, S.; Yang, C.; Tan, W., Aptamer-Based Detection of Circulating Targets for Precision Medicine. *Chem. Rev.* **2021**, 121, 12035–12105.
(4) Li, Y.; Liu, J., Aptamer-Based Strategies for Recognizing Adenine, Adenosine, ATP and Related Compounds. *Analyst* **2020**, 145, 6753-6768.
(5) Deng, J.; Walther, A., ATP-Responsive and ATP-Fueled Self-Assembling Systems and Materials. *Adv. Mater.* **2020**, 32, 2002629.
(6) Li, J.; Mo, L.; Lu, C.-H.; Fu, T.; Yang, H.-H.; Tan, W., Functional Nucleic Acid-Based Hydrogels for Bioanalytical and Biomedical Applications. *Chem. Soc. Rev.* **2016**, 45, 1410-1431.

(7) Biniuri, Y.; Luo, G. F.; Fadeev, M.; Wulf, V.; Willner, I., Redox-Switchable Binding Properties of the ATP-Aptamer. *J. Am. Chem. Soc.* **2019**, 141, 15567-15576.
(8) Xiong, Y.; Zhang, J. J.; Yang, Z. L.; Mou, Q. B.; Ma, Y.; Xiong, Y. H.; Lu, Y., Functional DNA Regulated CRISPR-Cas12a Sensors for Point-of-Care Diagnostics of Non-Nucleic-Acid Targets. *J. Am. Chem. Soc.* **2020**, 142, 207-213.
(9) Zhao, J.; Gao, J. H.; Xue, W. T.; Di, Z. H.; Xing, H.; Lu, Y.; Li, L. L., Upconversion Luminescence-Activated DNA Nanodevice for ATP Sensing in Living Cells. *J. Am. Chem. Soc.* **2018**, 140, 578-581.
(10) Sassanfar, M.; Szostak, J. W., An RNA Motif That Binds ATP. *Nature* **1993**, 364, 550-553.
(11) Huizenga, D. E.; Szostak, J. W., A DNA Aptamer That Binds Adenosine and ATP. *Biochemistry* **1995**, 34, 656-665.
(12) Dieckmann, T.; Butcher, S. E.; Sassanfar, M.; Szostak, J. W.; Feigon, J., Mutant ATP-Binding RNA Aptamers Reveal the Structural Basis for Ligand Binding. *J. Mol. Biol.* **1997**, 273, 467-478.
(13) Dieckmann, T.; Suzuki, E.; Nakamura, G. K.; Feigon, J., Solution Structure of an ATP-Binding RNA Aptamer Reveals a Novel Fold. *RNA* **1996**, 2, 628-640.
(14) Jiang, F.; Kumar, R. A.; Jones, R. A.; Patel, D. J., Structural Basis of RNA Folding and Recognition in an AMP-RNA Aptamer Complex. *Nature* **1996**, 382, 183-186.
(15) Lin, C. H.; Patel, D. J., Structural Basis of DNA Folding and Recognition in an AMP-DNA Aptamer Complex: Distinct Architectures but Common Recognition Motifs for DNA and RNA Aptamers Complexed to AMP. *Chem. Biol.* **1997**, 4, 817-832.
(16) Lyu, C.; Khan, I. M.; Wang, Z., Capture-SELEX for Aptamer Selection: A Short Review. *Talanta* **2021**, 229, 122274.
(17) Nutiu, R.; Li, Y., In Vitro Selection of Structure-Switching Signaling Aptamers. *Angew. Chem. Int. Ed.* **2005**, 44, 1061-1065.
(18) Rajendran, M.; Ellington, A. D., In Vitro Selection of Molecular Beacons. *Nucleic Acids Res.* **2003**, 31, 5700-5713.
(19) Nakatsuka, N.; Yang, K.-A.; Abendroth, J. M.; Cheung, K. M.; Xu, X.; Yang, H.; Zhao, C.; Zhu, B.; Rim, Y. S.; Yang, Y.; Weiss, P. S.; Stojanović, M. N.; Andrews, A. M., Aptamer–Field-Effect Transistors Overcome Debye Length Limitations for Small-Molecule Sensing. *Science* **2018**, 362, 319-324.
(20) Boussebayle, A.; Groher, F.; Suess, B., RNA-Based Capture-Selex for the Selection of Small Molecule-Binding Aptamers. *Methods* **2019**, 161, 10-15.
(21) Yu, H.; Luo, Y.; Alkhamis, O.; Canoura, J.; Yu, B.; Xiao, Y., Isolation of Natural DNA Aptamers for Challenging Small-Molecule Targets, Cannabinoids. *Anal. Chem.* **2021**, 93, 3172-3180.
(22) Qu, H.; Wang, L.; Liu, J.; Zheng, L., Direct Screening for Cytometric Bead Assays for Adenosine Triphosphate. *ACS Sensors* **2018**, 3, 2071-2078.
(23) Sazani, P. L.; Larralde, R.; Szostak, J. W., A Small Aptamer with Strong and Specific Recognition of the Triphosphate of ATP. *J. Am. Chem. Soc.* **2004**, 126, 8370-8371.
(24) Özalp, V. C.; Pedersen, T. R.; Nielsen, L. J.; Olsen, L. F., Time-Resolved Measurements of Intracellular ATP in the Yeast Saccharomyces Cerevisiae Using a New Type of Nanobiosensor. *J. Biol. Chem.* **2010**, 285, 37579-37588.

(25) Zhang, L.; Chaput, J. C., In Vitro Selection of an ATP-Binding Tna Aptamer. *Molecules* **2020**, 25, 4194.
(26) Fiorillo, M.; Ózsvári, B.; Sotgia, F.; Lisanti, M. P., High ATP Production Fuels Cancer Drug Resistance and Metastasis: Implications for Mitochondrial ATP Depletion Therapy. *Front. Oncol.* **2021**, 11.
(27) Simard, T.; Jung, R. G.; Di Santo, P.; Ramirez, F. D.; Labinaz, A.; Gaudet, C.; Motazedian, P.; Parlow, S.; Joseph, J.; Moreland, R.; Marbach, J.; Boland, P.; Promislow, S.; Russo, J. J.; Chong, A.-Y.; So, D.; Froeschl, M.; Le May, M.; Hibbert, B., Performance of Plasma Adenosine as a Biomarker for Predicting Cardiovascular Risk. *Clin. Transl. Sci.* **2021**, 14, 354-361.
(28) Liu, H.; Xia, Y., Beneficial and Detrimental Role of Adenosine Signaling in Diseases and Therapy. *J. Appl. Physiol.* **2015**, 119, 1173-1182.
(29) Huang, P.-J. J.; Liu, J., A DNA Aptamer for Theophylline with Ultrahigh Selectivity Reminiscent of the Classical RNA Aptamer. *ACS Chem. Biol.* **2022**, 17, 2121–2129.
(30) Huang, P.-J. J.; Liu, J., Selection of Aptamers for Sensing Caffeine and Discrimination of Its Three Single Demethylated Analog. *Anal. Chem.* **2022**, 94, 3142–3149.
(31) Schlosser, K.; Li, Y., A Versatile Endoribonuclease Mimic Made of DNA: Characteristics and Applications of the 8-17 RNA-Cleaving DNAzyme. *ChemBioChem* **2010**, 11, 866-879.
(32) Santoro, S. W.; Joyce, G. F., A General Purpose RNA-Cleaving DNA Enzyme. *Proc. Natl. Acad. Sci. U.S.A.* **1997**, 94, 4262-4266.
(33) Hermann, T.; Patel, D. J., Adaptive Recognition by Nucleic Acid Aptamers. *Science* **2000**, 287, 820-825.
(34) Zuker, M., Mfold Web Server for Nucleic Acid Folding and Hybridization Prediction. *Nucleic Acids Res.* **2003**, 31, 3406-3415.
(35) Slavkovic, S.; Johnson, P. E., Isothermal Titration Calorimetry Studies of Aptamer-Small Molecule Interactions: Practicalities and Pitfalls. *Aptamers* **2018**, 2, 45-51.
(36) Li, Y.; Liu, B.; Huang, Z.; Liu, J., Engineering Base-Excised Aptamers for Highly Specific Recognition of Adenosine. *Chem. Sci.* **2020**, 11, 2735-2743.
(37) Slavkovic, S.; Zhu, Y.; Churcher, Z. R.; Shoara, A. A.; Johnson, A. E.; Johnson, P. E., Thermodynamic Analysis of Cooperative Ligand Binding by the ATP-Binding DNA Aptamer Indicates a Population-Shift Binding Mechanism. *Sci. Rep.* **2020**, 10, 18944.
(38) Zhang, Z.; Oni, O.; Liu, J., New Insights into a Classical Aptamer: Binding Sites, Cooperativity and More Sensitive Adenosine Detection. *Nucleic Acids Res.* **2017**, 45, 7593-7601.
(39) Barbu, M.; Stojanovic, M. N., A Fresh Look at Adenosine-Binding DNA Motifs. *ChemBioChem* **2012**, 13, 658-660.
(40) Canoura, J.; Yu, H.; Alkhamis, O.; Roncancio, D.; Farhana, R.; Xiao, Y., Accelerating Post-SELEX Aptamer Engineering Using Exonuclease Digestion. *J. Am. Chem. Soc.* **2020**, 143, 805-816.
(41) Chenqi Niu, C. Z., and Juewen Liu, Capture-Selex of DNA Aptamers for Estradiol Specifically and Estrogenic Compounds Collectively. *Environ. Sci. Technol.* **2022**, 56, 17702–17711.
(42) Jenison, R. D.; Gill, S. C.; Pardi, A.; Polisky, B., High-Resolution Molecular Discrimination by RNA. *Science* **1994**, 263, 1425-1429.

(43) Liu, Y.; Liu, J., Selection of DNA Aptamers for Sensing Uric Acid in Simulated Tears. *Anal. Sens.* **2022**, 2, e202200010.
(44) Nutiu, R.; Li, Y., Structure-Switching Signaling Aptamers. *J. Am. Chem. Soc.* **2003**, 125, 4771-4778.
(45) Serec, K.; Babić, S. D.; Podgornik, R.; Tomić, S., Effect of Magnesium Ions on the Structure of DNA Thin Films: An Infrared Spectroscopy Study. *Nucleic Acids Res.* **2016**, 44, 8456-8464.
(46) Every, A. E.; Russu, I. M., Influence of Magnesium Ions on Spontaneous Opening of DNA Base Pairs. *J. Phys. Chem. B* **2008**, 112, 7689-7695.
(47) Perez Tobia, J.; Huang, P.-J. J.; Ding, Y.; Saran Narayan, R.; Narayan, A.; Liu, J., Machine Learning Directed Aptamer Search from Conserved Primary Sequences and Secondary Structures. *ACS Synth. Biol.* **2023**, 12, 186–195.
(48) Alkhamis, O.; Xiao, Y., Systematic Study of in Vitro Selection Stringency Reveals How to Enrich High-Affinity Aptamers. *J. Am. Chem. Soc.* **2023**, 145, 194-206.
(49) Wang, F.; Liu, X. Q.; Willner, I., DNA Switches: From Principles to Applications. *Angew. Chem. Int. Ed.* **2015**, 54, 1098-1129.
(50) Zhao, Y.; Zuo, X.; Li, Q.; Chen, F.; Chen, Y.-R.; Deng, J.; Han, D.; Hao, C.; Huang, F.; Huang, Y.; Ke, G.; Kuang, H.; Li, F.; Li, J.; Li, M.; Li, N.; Lin, Z.; Liu, D.; Liu, J.; Liu, L.; Liu, X.; Lu, C.; Luo, F.; Mao, X.; Sun, J.; Tang, B.; Wang, F.; Wang, J.; Wang, L.; Wang, S.; Wu, L.; Wu, Z.-S.; Xia, F.; Xu, C.; Yang, Y.; Yuan, B.-F.; Yuan, Q.; Zhang, C.; Zhu, Z.; Yang, C.; Zhang, X.-B.; Yang, H.; Tan, W.; Fan, C., Nucleic Acids Analysis. *Sci. China Chem.* **2021**, 64, 171-203.
(51) McConnell, E. M.; Cozma, I.; Mou, Q.; Brennan, J. D.; Lu, Y.; Li, Y., Biosensing with DNAzymes. *Chem. Soc. Rev.* **2021**, 50, 8954-8994.
(52) Yang, K.-A.; Pei, R.; Stojanovic, M. N., In Vitro Selection and Amplification Protocols for Isolation of Aptameric Sensors for Small Molecules. *Methods* **2016**, 106, 58-65.

For TOC graphics only